Original Research Paper

A Novel Weighted Integral Energy Functional (WIEF) Algorithm: Augmented Reality (AR) for Visualising the Blood Vessels in Breast Implant Surgeries

[1]**Taranjit Kaur,** [1]**Abeer Alsadoon,** [1]**Paul Manoranjan,**
[1]**P.W.C. Prasad,** [2]**Anand Deva,** [2]**Jeremy Hsu and** [3]**A. Elchouemi**

[1]*School of Computing and Mathematics, Charles Sturt University, Sydney, Australia*
[2]*Faculty of Medicine and Health Sciences, Macquarie University, Australia*
[3]*Walden University, USA*

Corresponding Author:
P.W.C. Prasad
School of Computing and
Mathematics, Charles Sturt
University, Sydney, Australia
Email:cwithana@studygroup.com

Abstract: The use of Augmented Reality (AR) for visualising blood vessels in surgery is still at the experimental stage and has not been implemented due to limitations in terms of accuracy and processing time. The AR also hasn't applied in breast surgeries yet. As there is a need for a plastic surgeon to see the blood vessels before he cuts the breast and before putting the implant, this paper aims to improve the accuracy of augmented videos in visualising blood vessels during Breast Implant Surgery. The proposed system consists of a Weighted Integral Energy Functional (WIFE) algorithm to increase the accuracy of the augmented view in visualising the occluded blood vessels that covered by fat in the operating room. The results on breast area shows that the proposed algorithm improves video accuracy in terms of registration error to 0.32 mm and processing time to 23 sec compared to the state-of-the-art method. The proposed system focuses on increasing the accuracy in augmented view in visualising blood vessels during Breast Implant Surgery as it reduces the registration error. Thus, this study concentrates on looking at the feasibility of the use of Augmented Reality technology in Breast Augmentation surgeries.

Keywords: Augmented Reality, Breast Augmentation, Surgical Planning, Wavelet Decomposition, Vascular Pulsation, Random Decision Forests

Introduction

Augmented Reality (AR) is defined as overlaying and integrating virtual information over the real-time perceptive environment which enables the user to manipulate and use the information in an intuitive manner (Inácio *et al*., 2017; Raja and Calvo, 2017). The AR technology has been successfully used in a range of medical procedures, providing additional information during surgery that is generally not accessible during the operating process (Pelargos *et al*., 2017). Many successful cases in different fields of medicine have been linked to and associated with better surgical planning, triggering an urgent search for tools to improve accuracy and performance during surgery (Alan *et al*., 2017). At present, pre-operative planning is an important part in all surgical procedures based on patient specific information, often using data obtained through medical imaging to ensure successful outcomes from the surgery (Ribeiro *et al*., 2015).

There is a significant range of procedure-specific AR technologies available in the medical field broadly categorized as video-based display, see-through display and projection-based display. In video-based displays, virtual images are superimposed onto a real-time video stream to create an augmented view for the surgeon. See-through display is used to overlay the virtual images on a translucent mirror for the direct view of the surgeon while the projection-based display is used to directly overlay virtual images onto the patient's body part which is undergoing surgery (Suenaga *et al*., 2013), Fig. 1.

Fig. 1: (a) Traditional Surgery, (b) Video-Guided and (c) AR guided; [These images are downloaded using Google search engine, the image is free to use, share or modify, even commercially]

The visualization of patient specific anatomical structures using AR during surgery helps the surgeon to perform the surgery at high levels of accuracy thus simplifying complex procedures (Suenaga *et al.*, 2015; Teber *et al.*, 2009). Surgical anatomy visualization is enhanced by visual cues obtained from the virtual data of the medical image (Kang *et al.*, 2014), increasing the surgeon's visual awareness of high-risk surgical targets (Puerto-Souza *et al.*, 2014). Therefore, it is important for surgeons to visualize the anatomical structures of the patient in the operating room to increase the accuracy in the surgery and to obtain the secure outcomes from the surgery. The AR hasn't applied in breast surgeries yet. As there is a need for a plastic surgeon to see the blood vessels before he cuts the breast and before putting the implant, the assistance of AR guided surgery would be beneficial in aiding the surgeons to visualize the blood vessels of the patient's mandibular region, where the surgeon would perform the cut.

This study is aiming towards helping the plastic surgeons to perform breast augmentation in a safe and accurate manner by making a pocket in the breasts for the implant without damaging major blood vessels. The AR hasn't applied in breast surgeries. As the AR hasn't applied yet in breast surgeries, the basic aim of this paper is to research available AR techniques for visualizing patients' anatomical structures, specifically blood vessels, during a range of surgical procedures. The work aims to identify the best technique which can be utilized for visualizing blood vessels in Breast Augmentation Surgery. Breast Augmentation surgery, also known as Augmentation Mammoplasty, was the most commonly performed cosmetic surgery procedure in 2011, inserting implants beneath the breasts to increase their size. For operative planning of such procedures, surgeons still rely on visual assessments and other subjective approaches due to a lack of objective evaluation tools (Georgii *et al.*, 2014).

The existing state-of-the-art method used a mechanism to determine the tumour affected areas by identifying textural and color patterns of tissue types during the surgery using AR. The limitation of this mechanism is that it cannot handle the contour leakage i.e., when there is weak or missing boundary data in images. This leakage is occurred due to the presence of noise from motion artifacts of the patient due to the body movement during the patient's respiration at surgery time. Thus, the presence of weak boundaries reduces the accuracy of the segmentation process which in turn affects the overall accuracy of the existing system. We propose a new mechanism to overcome the contour leakage problem. The experimental results reveal that the proposed scheme outperforms the state-of-the-art method in terms of registration accuracy and processing time.

Related Work

To generate an augmented view for visualising blood vessels in an operating room, a series of algorithms and techniques have been introduced that mainly focusing on accuracy and processing time. The AR systems, in which patient-specific information generated from pre-operative data is displayed intra-operatively, have been clinically applied in a range of surgical fields to enhance accuracy, safety and efficiency during surgery (Okamoto *et al.*, 2015). Kersten-Oertel *et al.* (2015) developed an AR system for neurovascular surgery to visualize internal anatomical structures such as blood vessels during surgery. It merges volume-rendered vessels with the live view of the patient in the operating room. The system uses filters to reduce the noise from the live video frames and a landmark registration protocol for increasing the accuracy of the generated augmented view. As visualization of the tumour in relation to its adjacent venous anatomy is crucial in neurosurgery, Low *et al.* (2010) developed an AR system for neurosurgical planning using Dextroscope and DEX-Ray platforms to present an augmented view that reveals the relationship of a patient tumor to its surrounding vessel structures during neurosurgery.

Cabrilo *et al.* (2014) proposed an AR system to visualize the anatomical structures during neurosurgery

surgeries. He utilized a neuro navigated workstation and microscope to operate on 28 patients with 39 unruptured aneurysms. Segmented vessel structures are introduced into the neuro navigated microscope and are superimposed on to the real patient. This hardware was used to provide an augmented view which makes the setup expensive. Kersten-Oertel *et al.* (2014) proposed an AR image-guided surgery system for neurosurgeons to visualize internal anatomical structures such as blood vessels during neurovascular surgery using OpenGL fragment shader. Virtual vessel volumes are merged with the live patient images using alpha blending.

In a different area of medicine, Hayashi *et al.* (2016) aimed to reduce the registration error for gastric cancer for surgical navigation during laparoscopic gastrectomy by using a weighted point-based registration technique by performing progressive internal landmark registration using internal anatomical fiducial to improve registration accuracy. However, the system uses internal anatomical landmarks and a 3D positional tracker for better registration. Similarly, Satoshi (Ieiri *et al.*, 2012) solved the problem of hidden vascular variations in endoscopic surgery. He developed an AR navigation system to increase accuracy for laparoscopic surgery by placing five multimodal markers on the patient's body to establish coordinates using optical tracking to increase accuracy. The optical tracking device is used to obtain the coordinates of each marker in the patient space. Then, a patient coordinate system is established.

Nicolau *et al.* (2011) analyzed available interactive and automatic AR systems in digestive surgical oncology in terms of current issues and future evolution of AR technology with the aim of integrating such technology in the operating room. He found the issues that still have to be tackled so that this technology can be seamlessly integrated in the operating room. As the lack of visibility of anatomical structures is a problem in gastrointestinal, hepatobiliary and pancreatic surgery, Sugimoto *et al.* (2010) provides a framework using non-invasive markerless registration with the help of physiological markers on the body surface. It used volume rendered preoperative data to project the information on to the body of the patient during Laparoscopy surgery in the operating room. The DICOM workstation used physiological markers on the patient's body for better registration. The Registration is between the patient's virtual body surface comprising the virtual umbilicus and the actual body surface by OsiriX.

Haouchine *et al.* (2013) proposed a method for real-time augmentation of the tumor and the vascular network with a laparoscopic view during liver surgery by considering the liver deformations and the tissue heterogeneity. A biomechanical model and a ray casting method is used to create the augmented view. However, surgical events such as smoke and bleeding can hamper

the tracking process in the system. Zhu *et al.* (2017) developed a navigation system to display inferior alveolar nerve bundles for maxillofacial surgery based on AR using a novel tracking and registration technique. The relationship between the virtual image and the real object is established by means of an occlusal splint attached to the fiducial marker. This is used to develop a relationship between marker and mandible during the real surgery, but unexpected errors can occur due to incorrect placement of the occlusal splint. Wang *et al.* (2017) presented a video-see through AR system by using Tracking Learning Detection (TLD) and Iterative Closet Point (ICP) algorithms. This work analyzed integral imaging with AR surgical navigation further using a 3D calibration algorithm which helps to reduce the initial registration error. Ulrich *et al.*'s (2012) method is a registration technique that resolves the initial alignment problem caused by manual adjustment and helps the automatic recovery. However, the system fails to provide depth perception in the augmented view. Ai *et al.* (2016) have proposed an augmented reality system for superimposing veins directly on the skin surface to visualize the exact location for accurate intravenous injections. A multiple-feature clustering method is used for the process of segmentation. However, the technique is unable to provide high-quality output.

Nosrati *et al.* (2016) introduced a system to augment an endoscopic view in the operating room with pre-operative 3D models. The major goal in developing the system was to develop a variational method to augment the endoscopic view of the surgeon by segmenting both visible and occluded structures encountered during the intraoperative endoscopic view. A wavelet decomposition technique is used to identify vascular pulsatile motion in the video frames, which helps with identifying occluded blood vessels hidden under fat tissue. The system used Random decision Forests (RF) to detect textual and color patterns of different tissue types present in the endoscopic scene such as that of a kidney and a tumor. However, the use of RF increased the overall complexity of the system and ultimately affected the processing time for creating the augmented view. The usability of the technique has been tested in fifteen challenging clinical cases, with a result of 45% improvement in system accuracy compared to other available AR systems. However, Nosrati *et al.* did not consider the problem of contour leakage which arises due to motion artifacts of the patient. The noise, which come from the breathing of the patient, deteriorates the object boundaries which makes it difficult to segment the desired objects, thus reducing the system accuracy. This problem, therefore, needs to be considered for further improvement to develop a more accurate AR system.

This paper takes the best features from the work of Nosrati *et al*. (2016) and focuses on increasing the system accuracy by removing the noise caused by patient respiration from the video frames The remainder of the paper is organized as follows: The section called "System Overview" describes the state-of-the-art method and details of the proposed technique including a system flowchart and pseudocode. The next section discusses result from the proposed technique and compares these with outcomes from the state-of-the-art method. The last section, discussion concludes the paper.

The current approach to AR in a range of surgical procedures is to use several techniques and algorithms to improve the accuracy and processing time of videos in visualising important anatomical structures. The highest current accuracy equates to a 0.87 mm overlay error (the difference between the projected scene and the actual scene) and processing time is 77 sec for generating the augmented view. Such overlay error (reduced accuracy) can lead to surgical failure.

Similarly, high processing time can delay the surgery (Nosrati *et al*., 2016).

State of Art Solution

The system was proposed by Nosrati *et al*. (2016) and delivers high accuracy in terms of visualizing blood vessels hidden by fat. It is also a cost-effective solution as there is no need for medical equipment such as markers that have been used in other current solutions. This solution has applied to Endoscopy Scenes for Kidney Surgery with the purpose of visualising the blood vessels, the tumour and the kidney (tissue patterns) in three different colours to diagnose the areas that are affected by the tumour. This solution used a variational technique, Wavelet Decomposition, which augments the endoscopic view (Live Video Frame) of the intraoperative environment. This technique identifies visible and occluded anatomical structures - blood vessels hidden by fat. This model consists of two key system stages Preoperative and intraoperative Fig. 2.

Fig. 2: Block Diagram of the State of Art System, Nosrati *et al*. (2016); [The blue borders show the good features of this state of art solution and the red border refers to the limitation of it]

Pre-operative Environment

The state of art (Nosrati *et al.*, 2016) process starts with segmenting the structures of interest from the 3D pre-operative data to create a 3D segmented model that can be aligned to the segmented 2D intraoperative data to provide an augmented view for the surgeon in the operating room during the endoscopic surgery. To deform the 3D pre-operative models of interest, intraoperative video frames are generalized using Eigen decomposition. Then, using these deformation models, the 3D pre-operative models are transformed.

Intra-operative Environment using Energy Functional Algorithm

In the intraoperative environment (Nosrati *et al.*, 2016), a real time video of the surface of the part of interest is recorded by the camera. Image frames are taken from the video. Then, Wavelet Decomposition technique divides each live video frame into four frequency sub-bands during the surgery. Blood vessel information is hidden in live video frames due to fat and noise that comes from surgical navigational tool – here, inserting the breast implant.

The main goal of the state of art (Nosrati *et al.*, 2016) is using the AR to diagnose the areas that affected by tumour. Along with this, Random decision Forests (RF) are trained and used to identify textural and color patterns of tissue types during the surgery. The RF help in classifying and distinguishing between different structures of interest, such as a tumor and a kidney. Subsequently, the energy functional is used to align and segment the preoperative data with the intraoperative data to create an augmented view in the operating room.

The state-of-the-art method (Nosrati *et al.*, 2016) provides accuracy with a registration error of 0.87 mm in visualizing patient anatomical structures. This can be improved to 0.32 mm using the proposed technique. The limitation of the state-of-the-art method is that segmentation of the live video frames is affected by contour leakage. Contour leakage occurs when there is weak or missing boundary data in images. The boundary definition deteriorates due to the presence of noise from motion artifacts of the patient due to respiration during surgery, where the patient's breathing causes movement in the physical body parts thereby creating noise in images taken during surgery. The presence of weak boundaries reduces the accuracy of the segmentation process which in turn affects the overall accuracy of the system. Moreover, the use of RF increases the complexity of the system because these are binary decision trees which are considered complex and increase processing time of the system. Also, the use of RF does not support depth perception because RF is trained from 2D endoscopic views to describe the probability of any pixel belonging to a certain structure of interest. Therefore, depth perception is not present in the use of RF in the process.

The state of art solution (Nosrati *et al.*, 2016) has considered the vessels, kidney and tumour as their purpose is to identify them in three different colours to diagnose the areas that are affected by the tumour. The accuracy of the state-of-the-art method depends on the type of segmentation in the intraoperative data. For segmentation, the Energy Functional technique is used. The Energy Functional (E) is calculated by the following Equation (1) (Nosrati *et al.*, 2016):

$$E(\Phi) = \sum_{n=1}^{N}\sum_{m=1}^{M} \int_{\Omega_{2D}^{m}} \left(2\rho_m^n - 1\right)(x) H\left(\phi_m^n(x)\right) dx \qquad (1)$$

where, $H(.)$ is the Heaviside function, $\rho_m^n(x)$ is the regional term for vessel, tumour and kidney structures; N represents the number of structures of interest; M represents the number of endoscopic images $\Phi = \left\{\phi_1^1,...,\phi_1^N,...,\phi_M^1,...,\phi_M^N\right\}$ represents the nth structure in the mth image, x is image pixels.

The patient is fully asleep throughout the surgery but generates breathing noises which are registered on the real time video that is taken throughout the surgery, reducing the accuracy of the segmentation process during surgery, which in turn affects the overall accuracy of the system.

Proposed Solution

There are a range of techniques available from different surgical fields which can be used to visualise patient-specific anatomical structures. Although no specific research has been done in relation to breast implant surgery, the existing techniques from other surgical fields have been reviewed to consider the feasibility of AR in visualising blood vessels during breast implant surgery. An analysis of advantages and disadvantages of each available method was carried out in this article. The major issues in relation to this technology are accuracy, processing time, depth perception and occlusion handling. From the techniques that were examined, one method was selected as the best model (Nosrati *et al.*, 2016) and has been used as a basis for the proposed solution. The useful features of the base model were enhanced with WIFE algorithm to overcome the limitation of contour leakage. Also, the use of RF is unable to support the depth perception. Therefore, RF will not be used in the proposed solution. The proposed system is presented in Fig. 3 and the pseudo code of it in Table 1. This paper proposes a new Weighted Integral Energy Functional (WIEF) algorithm to increase accuracy and to decrease processing time. The proposed

method increases accuracy by reducing the registration error from 0.87 to 0.32 mm in the augmented video in the operating room. Furthermore, processing time is improved from 77 to 23 sec using the proposed method.

Pre-operative Environment

From the techniques that were examined, one method was selected as the best model (Nosrati *et al.*, 2016) and has been used as a basis for the proposed solution. The useful features of the base model were enhanced with WIFE algorithm to overcome the limitation of contour leakage. Also, the use of RF is unable to support the depth perception. Therefore, RF will not be used in the proposed solution. The proposed system is presented in Fig. 3 and the pseudo code of it in Table 1. This paper proposes a new Weighted Integral Energy Functional (WIEF) algorithm to increase accuracy and to decrease processing time. The proposed method increases accuracy by reducing the registration error from 0.87 to 0.32 mm in the augmented video in the operating room. Furthermore, processing time is improved from 77 to 23 sec using the proposed method.

Intra-Operative Environment

The proposed WIEF algorithm focuses on the contour leakage problem by adding a filter and a weighted integral function into the current method. The noise present in the video frames is removed by applying a Gaussian Filter. Regularization controls the weak object boundaries. A Weighted Integral is also used in the proposed algorithm which acts as regularization for the object boundaries in the image where constant intensity is present to avoid the disappearance of the weak boundaries by stopping the contour from passing through the weak object boundaries. The proposed technique helps in segmenting object boundaries more accurately by considering their evolution over time, regulating the curve and reducing the effect of the noise from the image. In addition, the complexity of the system is reduced by removing the RF. RF in the state-of-the-art solution was used to learn textural and colour patterns of tissue types during surgery such as a tumour and a kidney, which is not required in the proposed solution as it focuses on visualizing the blood vassals in breast augmentation surgery, in which those tissue patterns are not required. Therefore, the complexity of the system due to the use of RF is reduced.

Proposed Equation

Let, $\phi_m^i : \Omega_{2D}^m \rightarrow \mathbb{R}$ be the level set function to represent the boundary of the ith structure in I_m endoscopic image. Using M camera views $I_m : \Omega_{2D}^m \subset \mathbb{R}^2 \rightarrow \mathbb{R}^3$ represent the

3-channel RGB image of the mth camera view. The proposed Weighted Integral Energy Functional E to align and segment the preoperative data with the intraoperative data is defined as Equation 2:

$$E(\Phi) = \sum_{n=1}^{N}\sum_{m=1}^{M} R_p\left(\phi_m^n\right) + E_{ext}\left(\phi_m^n\right) \tag{2}$$

where, $R_p(\Phi)$ is weighted regularization term that modified by us and given in Equation (3) and the $E_{ext}(\Phi)$ is external energy and enhanced by us and given in Equation (4) which are further defined as Equation 4:

$$R_p(\Phi) = \int_{\Omega_{2D}^m} p\left(|\nabla\phi|^p\right) dx\, dy \tag{3}$$

where, p is potential function $p:[1,\infty) \rightarrow \mathbb{R}$ helps in keeping level set function close by the signed distance function. The local property of image is not reflected by the exponent p because it is constant. Therefore, it acts as regularization for the object boundaries in the image where constant intensity is present to avoid the disappearance of the weak boundaries by stopping the contour to pass through the weak object boundaries.

Table 1: Proposed System with WIEF algorithm

Algorithm: Proposed method
Input: 2D Intraoperative data
Output: 3D Augmented View

BEGIN
Step-1: Wavelet decomposition of the video frames is performed to obtain the vascular pulsatile motion in the patient.
Step-2: Remove noise using Laplacian of Gaussian filter from the video frame.
Step-3: Calculate the energy functional of the intraoperative data.

$$E_{ext}(\Phi) = \int_{\Omega_{2D}^m} \left(\nabla G_\sigma * I_m\right)\left(2\rho_m^v - 1\right)(x) H\left(\phi_m^n(x)\right) dxdy$$

where, ∇G_σ Laplacian of Gaussian filter with standard deviation σ

ρ_m^v represents the regional appearance of blood vessels

$H(.)$ is the Heaviside function
Step-4: Apply Weighted regularization function.

$$R_p(\Phi) = \int_{\Omega_{2D}^m} p\left(|\nabla\phi|^p\right) dx\, dy$$

where, p is potential function $p:[1,\infty) \rightarrow \mathbb{R}$ helps in keeping level set function close by the signed distance function
Step-5: Calculate the Weighted Integral Energy Functional E to align and segment the preoperative data with the intraoperative data

$$E(\Phi) = \sum_{n=1}^{N}\sum_{m=1}^{M} R_p\left(\phi_m^n\right) + E_{ext}\left(\phi_m^n\right)$$

where, $R_p(\Phi)$ is the weighted regularization term and $E_{ext}(\Phi)$ is external energy calculated in Step-3 and Step-4, respectively.
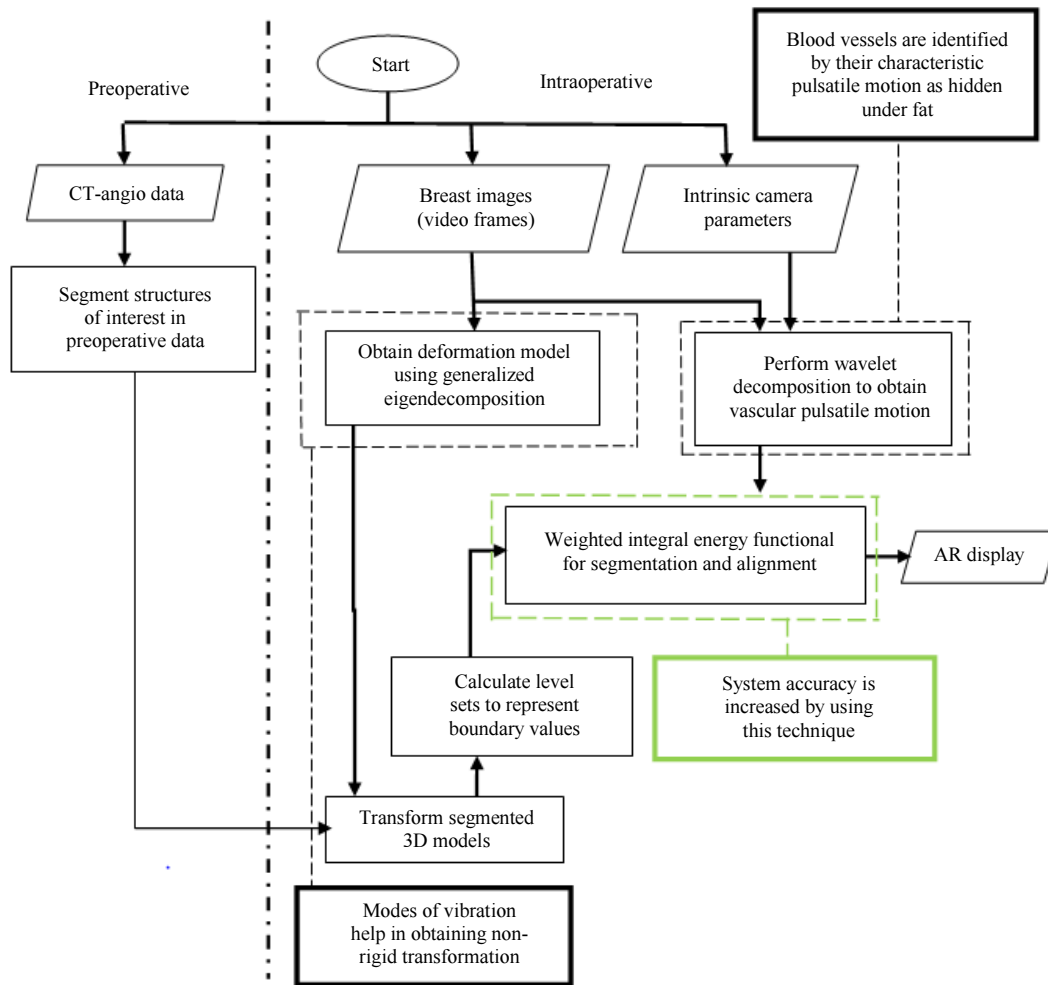END

Fig. 3: Block diagram of the proposed AR system for Breast Implant Surgery Using Weighted Integral Energy Functional (WIEF) algorithm; [The green borders refer to the new parts in our proposed system]

The $E_{ext}(\Phi)$ is the enhanced external energy which is defined in order to transfer the zero-level curve near the object boundaries as Equation 4:

$$E_{ext}(\Phi) = \int_{\Omega^m_{2D}} (\nabla G_\sigma * I_m)(2\rho^v_m - 1)(x) H(\phi^n_m(x)) dx\, dy \qquad (4)$$

where, ∇G_σ Laplacian of Gaussian filter with standard deviation σ. The Gaussian kernel with standard deviation σ is used to remove noise from the image and the Laplace operator detects the edges from the image. The object boundaries are defined in the image where opposite flow encounters using the Laplacian of Gaussian filter. Term ρ^v_m represents the regional appearance of blood vessels which are hidden under fat and are detected by using the vascular pulsatile motion; other regional terms used in the state-of-the-art method for kidney and tumour are not used in the proposed technique as those terms are irrelevant in the context and

$H(.)$ is the Heaviside function. Therefore, the motion of the curve towards the desired object boundaries is derived by the external energy term.

The technique of Energy Functional present in the state-of-the-art solution is unable to provide high accuracy due to a contour leakage problem. In contrast, the proposed technique, given in Equation (1), helps in segmenting object boundaries more accurately by considering their evolution over time by regulating the curve using the weighted integral $R_p(\Phi)$ and reducing the effect of the noise from the image using the ∇G_σ Laplacian of Gaussian filter. Moreover, the complexity of the system is reduced by removing the RF.

Experimental Validation

Matlab R2017a has been used for the implementation of the proposed system. To generate the results, sets of 10 sample videos and 10 sample CT scan images from

patients from different age groups and body mass were used with results represented in Table 2. A range of online resources have been used to gather the sample images and videos. We have used a range of measures to compare the performance, for example, the registration overlay error, processing time and visualized blood vessel in the samples. The registration error is determined using Matlab tools by considering pixel differences and then converting it into the distance in terms of mm. The processing time is determined by recoding the time of the execution of the algorithms. We also provide visualizations of the blood vessels to show the effectiveness of the proposed scheme. The measures clearly demonstrate the performance comparisons with physical meaning of improvement. Since Matlab was used for the simulation, the image overlayed in the AR video differs somewhat from real experimental results. In Table 2, the original volume refers to the preoperative information from patients utilised to segment the structures of interest. The proposed system was applied to the video frames and the result is shown in Table 2 with the red lines representing the visualised blood vessels shown in the processed samples.

The original volume utilised in the preoperative environment is shown in the Fig. 4a. In the intraoperative environment, a camera captures continuous 2D video images (real time video) of the patient's breasts and converts these into video frames. Figure 4b shows a sample of the vascular pulsation which identifies the occluded blood vessels using wavelet decomposition. Then, the Gaussian filter is applied to these video frames to remove the noise which is generated from patient's breathing during the surgery. The Gaussian filter helps in reducing the edge blurring and it is also computationally faster. The required degree of accuracy is provided by this filter; therefore, no other filter has been used. This filter highlights regions of rapid intensity change in an image and is capable of preserving the edge and removing the noise. Other techniques were not considered as this filter provides the expected accuracy for our purpose.

The proposed enhanced energy functional is used to derive the motion of the curve towards the desired object boundaries. It aligns the pre-operative 3D data with the 2D intra-operative data for this purpose. The modified weighted regularization is used to remove the contour leakage by regulating the curve and reducing the effect of the noise from the image. Thus, the proposed weighted integral energy functional, which includes *modified weighted regularization and enhanced energy functional,* helps in segmenting the object boundaries more accurately by considering their evolution over time. It regulates the boundary curve and reduces the effect of the noise coming from the image using the Laplacian of the Gaussian filter. Random decision forests were not used in our proposed solution as there is no need to classify and distinguish the tissue patterns as the plastic surgeon does require visualisation of the blood vessels. This has reduced the processing time of the proposed system. The intraoperative data is aligned to the preoperative data to generate the augmented view for the surgeon. The processed sample is shown in Fig. 4c.

Computing the term ρ^y depending upon appearance alone is difficult as blood vessels are typically hidden under fat. However, these can be identified by their characteristic pulsation motion, which is invisible to the naked eye but is detectable. Therefore, the vascular pulsation motion analysis is important to produce the ρ^y term.

The difference in accuracy and processing time between the proposed solution and the state of art is shown below. The results for accuracy from the breast samples are discussed in Fig. 5 and in Fig. 6 in terms of processing time. Image registration is the process of matching two different objects based on reference points. It is used in intra-surgery to align a preoperative 3D model with 2D images from the surgery, requiring reference points for image alignment. The images need to be registered in order to achieve the alignment. The reference points of the 2D images were defined manually using Matlab, so that registration could be carried out using vascular pulsation cues. This aids the preoperative to intraoperative alignment process allowing for both rigid and heterogeneous physically based, patient-specific non-rigid deformations.
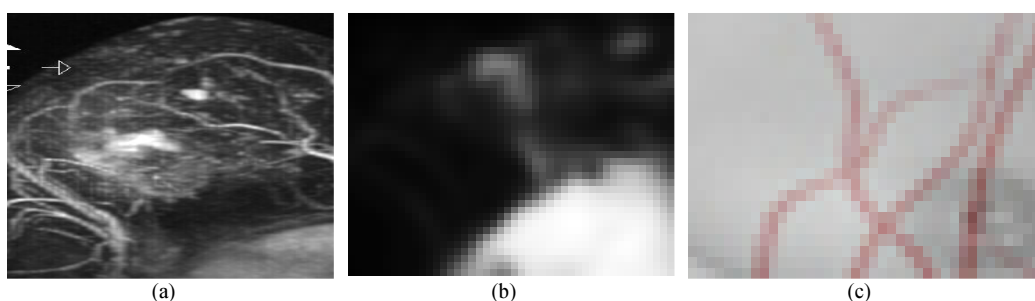

Fig. 4: (a) Original Volume (b) Vascular Pulsation (c) Processed Sample
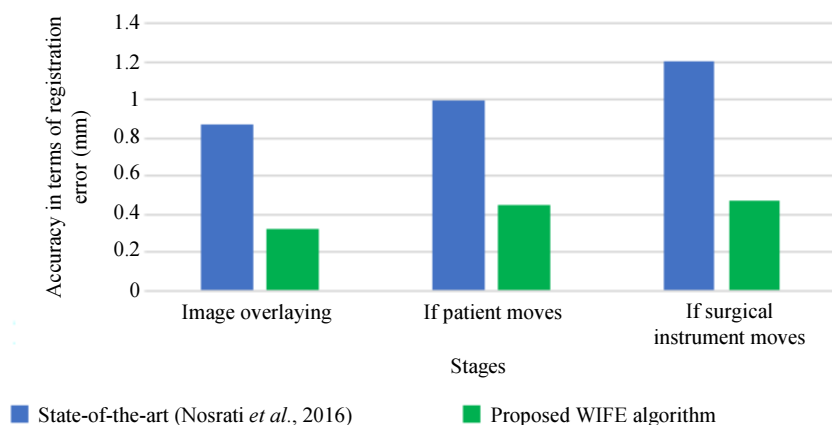
Fig. 5: Results of accuracy comparisons between the sate of art and proposed solutions (smaller value of registration error indicates better accuracy)
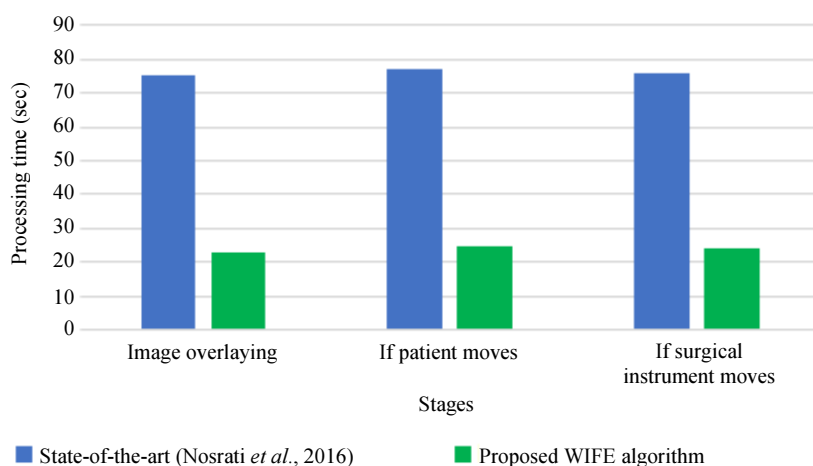

Fig. 6: Results of processing time comparisons between the sate of art and proposed solutions (smaller value of processing time indicates better performance)
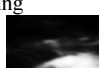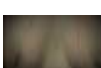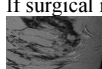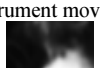
The subjects in the collected data set range in age from 21 to 53 and in weight from 100lb to 190lb. Different breast sizes were considered to produce the results for both, the state-of-the-art and the proposed method. Accuracy in terms of registration error and the processing time in terms of seconds were the parameters used to measure the system performance. The registration error is measured as the root mean square distance between corresponding points. The graphs comparing the performance parameters for the state-of-the-art and the proposed method are represented. The accuracy comparison is shown in Fig. 5, with the blue bar indicating the registration error in the current method and the green bar in the proposed method: lower value of the registration error equates to higher accuracy. The system configuration is described here as follows: The system used for running the simulation was Pentium(R) Dual-Core CPU T4300 @ 2.10GHz with 4 GB installed

memory. The system was Windows 7 Ultimate, 64-bit operating system. The processing time is shown in Fig. 6, where again the blue bar indicates the absolute processing time in the current method and the green bar in the proposed method and the lower value of the processing time equates to better performance of the system. However, this above-mentioned processing time may vary with the changes in the system configuration. If processor (CPU) and other system internal features are changed, then this time can vary. So, if RAM is increased processing time will be reduced and vice-versa. Note that the registration/alignment is manual, by matching point by point using a third-party software. The number of reference point choices have influenced in the time calculation. However, we have used the same procedure for both algorithms, thus, the comparative picture in terms of computational time should remain the same.

Table 2: Results for accuracy and processing time of visualising the breast blood vessels of proposed and state of art solutions

S. no	Sample details	Original volume	Pulsation using Wavelet	State of Art (Nosrati *et al.*, 2016)			Proposed solution		
				Processed sample	Accuracy by Registration Error	Processing Time	Processed sample	Accuracy by Registration Error	Processing Time
1	Breasts	Image overlaying							
	(31, 5'6", 140)				0.9 mm	80 sec		0.35 mm	23 sec
		If patient moves							
					1 mm	82 sec		0.37 mm	25 sec
		If surgical instrument moves							
					1 mm	81 sec		0.35 mm	25 sec
2	Breasts	Image overlaying							
	(34, 5'2", 190)				1.3 mm	79 sec		0.30 mm	21 sec
		If patient moves							
					1.7 mm	77 sec		0.32 mm	22 sec
		If surgical instrument moves							
					1.75 mm	79 sec		0.30 mm	21 sec
3	Breasts	Image overlaying							
	(40, 5'7", 155)				1.89 mm	80 sec		0.45 mm	23 sec
		If patient moves							
					1.92 mm	78 sec		0.39 mm	20 sec
		If surgical instrument moves							
					1.90 mm	79 sec		0.37 mm	22 sec
4	Breasts	Image overlaying							
	(25, 5'2", 120)				1.86 mm	88 sec		0.29 mm	30 sec
		If patient moves							
					1.88 mm	87 sec		0.28 mm	27 sec
		If surgical instrument moves							
					1.99 mm	88 sec		0.22 mm	28 sec
5	Breasts	Image overlaying							
	(46, 5'8", 142)				1 mm	78 sec		0.31 mm	20 sec
		If patient moves							
					1.2 mm	79 sec		0.32 mm	22 sec
		If surgical instrument moves							
					1.2 mm	79 sec		0.32 mm	23 sec
6	Breasts	Image overlaying							
	(25, 5'3", 160)				0.98 mm	75 sec		0.24 mm	25 sec
		If patient moves							
					1 mm	77 sec		0.30 mm	22 sec

Table 2: Continu

#	Breasts	Condition	Original	Error	Time	Proposed	Error	Time
7	Breasts (45, 5'3", 116)	If surgical instrument moves		1 mm	72 sec		0.31 mm	27 sec
		Image overlaying		0.89 mm	70 sec		0.32 mm	23 sec
		If patient moves		0.90 mm	72 sec		0.30 mm	25 sec
		If surgical instrument moves		0.88 mm	70 sec		0.30 mm	22 sec
8	Breasts (48, 5'1", 115)	Image overlaying		0.75 mm	80 sec		0.28 mm	25 sec
		If patient moves		0.80 mm	79 sec		0.29 mm	23 sec
		If surgical instrument moves		0.81 mm	81 sec		0.27 mm	26 sec
9	Breasts (53, 5'6", 120)	Image overlaying		0.73 mm	69 sec		0.32 mm	20 sec
		If patient moves		0.88 mm	72 sec		0.35 mm	22 sec
		If surgical instrument moves		0.89 mm	73 sec		0.40 mm	22 sec
10	Breasts (21, 5'4", 100)	Image overlaying		0.75 mm	74 sec		0.29 mm	21 sec
		If patient moves		0.89 mm	79 sec		0.30 mm	25 sec
		If surgical instrument moves		0.88 mm	79 sec		0.29 mm	23 sec

Gold Standard: AR is at present used in a variety of surgical procedures involving a range of techniques and algorithms to improve the accuracy and processing time of videos in visualising anatomical structures. The highest accuracy so far generated is 0.87 mm of overlay error (the difference between the projected scene and the actual scene) and processing time is 77 sec for generating the augmented view. Such overlay error (reduced accuracy) can lead to surgical failure. Similarly, high processing time can delay the surgery (Nosrati *et al*., 2016).

Results show major differences in accuracy and processing time between the State-of-the-Art system and the proposed system in terms of image overlay, when the patient moves and when surgical instruments move. In Table 2, the original volume refers to the preoperative information of the patient that is utilised to segment the structures of interest. The result of the proposed algorithm shows the video accuracy in terms of registration error as 0.32 mm and processing time as 23 sec compared to the state-of-the-art method which had a registration error of 0.87 mm and a processing time of 77 sec.

Conclusion

The AR system for visualising blood vessels in Breast Implant surgery can be created with a combination of different techniques. The energy functional has been enhanced by adding Gaussian filter to the Wavelet Decomposition technique to remove noise and detect the

desired boundaries. The weighted regularization was modified and used to overcome the contour leakage problems. This leads to greater accuracy in object boundaries segmentation as a consequence of considering their evolution over time. Thus, the proposed Weighted Integral Energy Functional, which includes modified weighted regularization and Enhanced Energy functional, helps in segmenting object boundaries more accurately by considering their evolution over time.

Although a range of techniques are available to create an AR visualization, they have so far failed to provide the required accuracy and processing time. These are the major factors that affect the use of AR during surgery. This research has explored opportunities for overcoming the limitations of the state of art solution. The proposed technique improves outcomes by segmenting object boundaries more accurately through considering their evolution over time by regulating the curve and reducing the effect of the noise from the image. Therefore, the accuracy of the proposed system in terms of registration error is reduced to 0.32mm.

Acknowledgement

Author's Contributions

Taranjit Kaur: He has completed this project as part of his MIT degree program.

Abeer Alsadoon: Worked on the setup of the experiments and gave important suggestions on design of experiments. In addition to, as Abeer Alsadoon is the main supervisor on this work that she provided the details guidelines and feedback in each step of this work.

Paul Manoranjan and P.W.C. Prasad: Made important revisions to most sections of the paper.

Anand Deva and Jeremy Hsu: Providing the idea of the topic and helped in modifying some parts.

A. Elchouemi: Give the final review and approval for the manuscript to be submitted.

References

Ai, D., J. Yang, J. Fan, Y. Zhao and X. Song *et al.*, 2016. Augmented reality based real-time subcutaneous vein imaging system. Biomed. Opt. Express, 7: 2565. DOI: 10.1364/BOE.7.002565

Alan, S., M. Herford and F. Miller, 2017. The use of virtual surgical planning and navigation in the treatment of orbital trauma - The use of virtual surgical planning and navigation in the treatment of orbital trauma. Chinese J. Trauma: English Edit., 20: 9-13. DOI: 10.1016/j.cjtee.2016.11.002

Cabrilo, I., P. Bijlenga and K. Schaller, 2014. Augmented reality in the surgery of cerebral aneurysms: A technical report. Neurosurgery, 10: 252-261. DOI: 10.1227/NEU.0000000000000328

Georgii, J., M. Eder, K. Burger, S. Klotz and F. Ferstl *et al.*, 2014. A computational tool for preoperative breast augmentation planning in aesthetic plastic surgery. IEEE J. Biomed. Health Inform., 18: 907-919. DOI: 10.1109/JBHI.2013.2285308

Haouchine, N., J. Dequidt, I. Peterlik, E. Kerrien and M.O. Berger *et al.*, 2013. Image-guided simulation of heterogeneous tissue deformation for augmented reality during hepatic surgery. Proceedings of the IEEE International Symposium on Mixed and Augmented Reality, Oct. 1-4, IEEE Xplore Press, Adelaide, SA, Australia, pp: 199-208. DOI: 10.1109/ISMAR.2013.6671780

Hayashi, Y., K. Misawa, D. Hawkes and K. Mori, 2016. Progressive internal landmark registration for surgical navigation in laparoscopic gastrectomy for gastric cancer. Int. J. Comput. Assisted Radiol. Surgery, 11: 837-845. DOI: 10.1007/s11548-015-1346-3

Ieiri, S., M. Uemura, K. Konishi, R. Souzaki and Y. Nagao *et al.*, 2012. Augmented reality navigation system for laparoscopic splenectomy in children based on preoperative CT image using the optical tracking device. Pediatric Surgery Int., 28: 341-346. DOI: 10.1007/s00383-011-3034-x

Inácio, J., J. Ribeiro, J. Campos, S. Silva and V. Alves, 2017. Augmented reality in surgery. Next-Generation Mobile and Pervasive Healthcare Solutions.

Kang, X., M. Azizian, E. Wilson, K. Wu and A. Martin *et al.*, 2014. Stereoscopic augmented reality for laparoscopic surgery. Endoscopic Surgery, 28: 2227-2235. DOI: 10.1007/s00464-014-3433-x

Kersten-Oertel, M., I. Gerard, S. Drouin, K. Mok and D. Sirhan *et al.*, 2015. Augmented reality in neurovascular surgery: feasibility and first uses in the operating room. Int. J. Comput. Assisted Radiol. Surgery, 10: 1823-1836. DOI: 10.1007/s11548-015-1163-8

Kersten-Oertel, M., I. Gerard, S. Drouin, K. Mok and D. Sirhan *et al.*, 2014. Augmented reality in neurovascular surgery: first experiences. Proceedings of the 9th International Workshop on Augmented Environments for Computer-Assisted Interventions, Sept. 14-14, Springer, Boston, MA, USA, pp: 80-89. DOI: 10.1007/978-3-319-10437-9_9

Low, D., C.K. Lee, L.L.T. Dip, W.H. Ng and B.T. Ang *et al.*, 2010. Augmented reality neurosurgical planning and navigation for surgical excision of parasagittal, falcine and convexity meningiomas. Brit. J. Neurosurgery, 24: 69-74. DOI: 10.3109/02688690903506093

Nicolau, S., L. Soler, D. Mutter and J. Marescaux, 2011. Augmented reality in laparoscopic surgical oncology. Surgical Oncol., 20: 189-189. DOI: 10.1016/j.suronc.2011.07.002

Nosrati, M., A. Amir-Khalili, J.M. Peyrat, J. Abinahed and O. Al-Alao *et al.*, 2016. Endoscopic scene labeling and augmentation using intraoperative pulsatile motion and color appearance cues with pre-operative anatomical priors. Int. J. Comput. Assisted Radiol. Surgery, 11: 1409-1418. DOI: 10.1007/s11548-015-1331-x

Okamoto, T., S. Onda, K. Yanaga, N. Suzuki and A. Hattori, 2015. Clinical application of navigation surgery using augmented reality in the abdominal field. Official J. Japan Surgical Society, 45: 397-406. DOI: 10.1007/s00595-014-0946-9

Pelargos, P.E., D.T. Nagasawa, C. Lagman, S. Tenn and J.V. Demos *et al.*, 2017. Utilizing virtual and augmented reality for educational and clinical enhancements in neurosurgery. J. Clin. Neurosci., 35: 1-4. DOI: 10.1016/j.jocn.2016.09.002

Puerto-Souza, G.A., J.A. Cadeddu and G.L. Mariottini, 2014. Toward long-term and accurate augmented-reality for monocular endoscopic videos. IEEE Trans. Biomed. Eng., 61: 2609-2620. DOI: 10.1109/TBME.2014.2323999

Raja, V. and P. Calvo, 2017. Augmented reality: An ecological blend. Cognitive Syst. Res., 42: 58-72. DOI: 10.1016/j.cogsys.2016.11.009

Ribeiro, J., V. Alves, S. Silva and J. Campos, 2015. A 3D Computed Tomography Based Tool for Orthopedic Surgery Planning. In: Developments in Medical Image Processing and Computational Vision, Tavares J. and R. Natal Jorge (Eds.), Springer, Cham, pp: 121-137.

Suenaga, H., H. Liao, K. Masamune, T. Dohi and K. Hoshi *et al.*, 2015. Vision-based markerless registration using stereo vision and an augmented reality surgical navigation system: A pilot study. BMC Med. Imag., 15: 51-51. DOI: 10.1186/s12880-015-0089-5

Suenaga, H., H.H. Tran, H. Liao, K. Masamune and T. Dohi *et al.*, 2013. Real-time in situ three-dimensional integral videography and surgical navigation using augmented reality: A pilot study. Int. J. Oral Sci., 5: 98-102. DOI: 10.1038/ijos.2013.26

Sugimoto, M., H. Yasuda, K. Koda, M. Suzuki and M. Yamazaki *et al.*, 2010. Image overlay navigation by markerless surface registration in gastrointestinal, hepatobiliary and pancreatic surgery. J. Hepato-Biliary-Pancreatic Sci., 17: 629-636. DOI: 10.1007/s00534-009-0199-y

Teber, D., S. Guven, T. Simpfendörfer, M. Baumhauer and E.O. Güven *et al.*, 2009. Augmented reality: A new tool to improve surgical accuracy during laparoscopic partial nephrectomy? Preliminary *in vitro* and *in vivo* results. Eur. Urol., 56: 332-332. DOI: 10.1016/j.eururo.2009.05.017

Ulrich, M., C. Wiedemann and C. Steger, 2012. Combining scale-space and similarity-based aspect graphs for fast 3D object recognition. IEEE Trans. Patt. Anal. Mach. Intell., 34: 1902-1902. DOI: 10.1109/TPAMI.2011.266

Wang, J., H. Suenaga, L. Yang, E. Kobayashi and I. Sakuma, 2017. Video see-through augmented reality for oral and maxillofacial surgery. Int. J. Med. Robot. Comput. Assisted Surgery. DOI: 10.1002/rcs.1754

Zhu, M., F. Liu, G. Chai, J. Pan and T. Jiang *et al.*, 2017. A novel augmented reality system for displaying inferior alveolar nerve bundles in maxillofacial surgery. Scientific Reports, 7: 42365-42365. DOI: 10.1038/srep42365